AIP | Applied Physics Letters

Evidence for enhanced ferromagnetism in an iron-based nanoglass

R. Witte, T. Feng, J. X. Fang, A. Fischer, M. Ghafari et al.

Citation: Appl. Phys. Lett. **103**, 073106 (2013); doi: 10.1063/1.4818493
View online: http://dx.doi.org/10.1063/1.4818493
View Table of Contents: http://apl.aip.org/resource/1/APPLAB/v103/i7
Published by the AIP Publishing LLC.

Evidence for enhanced ferromagnetism in an iron-based nanoglass

R. Witte,[1,2,a)] T. Feng,[1] J. X. Fang,[1] A. Fischer,[1] M. Ghafari,[1] R. Kruk,[1] R. A. Brand,[1] D. Wang,[1] H. Hahn,[1,2] and H. Gleiter[1]
[1]*Institute for Nanotechnology, Karlsruhe Institute of Technology (KIT), 76344 Eggenstein-Leopoldshafen, Germany*
[2]*Joint Research Laboratory Nanomaterials, Technische Universität Darmstadt, Petersenstr. 32, 64287 Darmstadt, Germany*

(Received 4 March 2013; accepted 29 July 2013; published online 13 August 2013)

The possibility to synthesize bulk amorphous materials with an internal nanostructure—nanoglasses—leads to yet another class of materials potentially with modified properties. Here, evidence is presented that the nanoglass model system $Fe_{90}Sc_{10}$ exhibits enhanced magnetic properties: it is shown that this nanoglass (prepared by cold compaction of glassy nanospheres) is a *ferromagnet* at ambient temperature although the isolated nanospheres are *paramagnetic*. Structural studies reveal that it consists of glassy nanospheres connected by regions with reduced atomic density. The ferromagnetism is explained by the presence of such regions of low atomic density. © *2013 AIP Publishing LLC*. [http://dx.doi.org/10.1063/1.4818493]

Modifying solid materials by the introduction of a high density of interfaces (grain boundaries), denoted nanocrystalline materials, is known to result in remarkable variations of properties compared to traditional structures.[1] An analogous approach for amorphous materials—nanoscale amorphous regions separated by a network of internal interfaces—has been proposed and such materials are referred to as "nanoglass".[2] A first structural study in the alloy system $Pd_{70}Fe_3Si_{27}$ indicated that such a heterogeneous amorphous structure is formed when nanometer-sized glassy droplets are compacted. In the as-compacted state, nanoglasses consist of nanometer-sized glassy regions separated by "interfaces." These interfaces were found to have a reduced density and a wider distribution of nearest neighbor interatomic spacings as compared to a conventional melt-spun glass.[2]

Recently, evidence for the existence of such interfaces in compacted nanoparticle materials has been obtained from a combined study of positron annihilation lifetime spectroscopy and small angle X-ray scattering,[3] as well as from a study applying high energy X-ray diffraction.[4] Molecular dynamics simulations have also provided evidence for internal glass-glass interfaces in a $Cu_{64}Zr_{36}$ metallic glass. These interfaces are characterized—in contrast to the melt spun glass—by a different short-range order with an enhanced free volume.[5,6] A recent study addressing the magnetic properties has demonstrated an itinerant component in the (low temperature) magnetically ordered state of a FeSc nanoglass.[7] However, to date, no definite experimental evidence of important property changes related to such interfaces in amorphous materials has been reported, which is the subject of this communication.

In this study, we report on a nanoglass with magnetic (and probably other density-related) properties differing significantly from those of the conventional amorphous counterpart with identical chemical composition, i.e., a glass produced by melt-spinning. The nanoglass was prepared by consolidating ~10 nm-sized glassy (amorphous) spheres of $Fe_{90}Sc_{10}$ previously produced by inert gas evaporation/condensation.[8] Disc-shaped samples (diameter ~8 mm) were formed by *in-situ* compaction at 1.5 GPa, followed by *ex-situ* compaction at 4.5 GPa. Magnetic properties were characterized using SQUID (Superconducting Quantum Interference Device) magnetometry and Mössbauer spectroscopy (MS). Moreover, their structure was studied by MS as well as scanning tunneling microscopy (STM).

Figure 1 presents the room temperature (RT) magnetization loops, M (magnetization) vs. H (external magnetic field), of a $Fe_{90}Sc_{10}$ nanoglass sample and of a melt-spun ribbon with the same composition. (Elemental analysis was performed using energy-dispersive X-ray spectroscopy, not shown here.) It is evident that the ribbon is paramagnetic at RT, in agreement with literature.[9,10] In contrast, the $Fe_{90}Sc_{10}$ nanoglass is ferromagnetic and reaches an average magnetization of about 1.05(1) μ_B per Fe atom. However, note that even at 4 T, the magnetization of the nanoglass is not fully saturated.

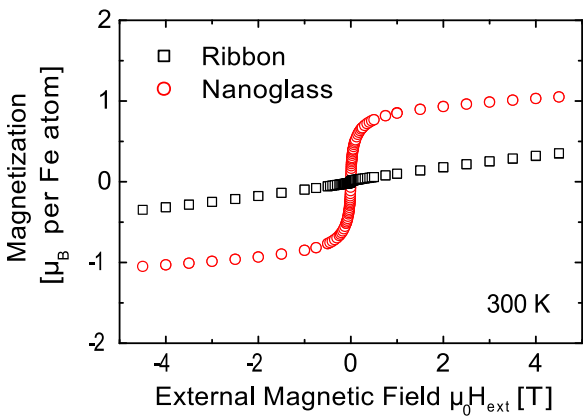

FIG. 1. Magnetization curves for a nanoglass sample and a melt-spun ribbon at 300 K. The ribbon exhibits a paramagnetic behavior, while the nanoglass shows a ferromagnetic shape reaching a magnetization of 1 μ_B per Fe atom in the applied magnetic field of 4.5 T.

[a)]Author to whom correspondence should be addressed. Electronic mail: ralf.witte@partner.kit.edu

In order to identify the origin of the ferromagnetism, the structural details of the nanoglass and of the melt-spun ribbon were analyzed using STM and MS. STM images of the polished surfaces (Fig. 2(a) of the ribbon and Fig. 2(b) of the nanoglass) illustrate the different nanostructures. The ribbon sample shows some modulation on a scale of about 2 to 5 nm but no clearly discernible clusters. The nanoglass sample possesses a different structure: there is a definite cluster-like modulation on the same scale as the original nanoparticles. This proves that the granular structure is retained after consolidation. A nanostructure such as shown in Fig. 2(b) has never been reported in the literature for an amorphous bulk-like sample. Only in thin amorphous films, a nano-granular structure has been observed (e.g. Refs. 11–13). The granular appearance seen in the STM image is indicative of interfaces formed between the amorphous nanoparticles. The STM image of the ribbon surface, presented in Fig. 2(a), displays only local fluctuations on a smaller length scale, as has been reported for other melt-spun samples (e.g. Ref. 14).

Further information about the local environment and magnetic state of ^{57}Fe-probe atoms is provided by MS. The results at RT are presented in Figs. 2(c)–2(e). The single line spectrum from the ribbon, Fig. 2(c), is consistent with a paramagnetic state as was shown in Fig. 1. The same type of spectrum was obtained for the isolated nanometer-sized $Fe_{90}Sc_{10}$ glassy spheres (Fig. 2(d)) prior to compaction. In striking contrast, the spectrum of the nanoglass, Fig. 2(e), was found to consist of two components. In fact, the spectrum may be fitted by (i) a paramagnetic component similar to that of the ribbon (Fig. 2(c)) or the isolated $Fe_{90}Sc_{10}$ nanospheres (Fig. 2(d)) and (ii) a ferromagnetic component (six line sub-spectrum: red, continuous line in Fig. 2(e)). The presence of two sub-spectra (ferromagnetic and paramagnetic) indicates that the magnetic structure of the $Fe_{90}Sc_{10}$ nanoglass is heterogeneous. There are simultaneously regions that are magnetically disordered (single line) and others that are magnetically ordered (six line sub-spectrum).

It should be noted that ferromagnetic order has never been observed at RT in melt-spun and vapor-deposited amorphous Fe_xSc_{100-x} alloys over the whole compositional range. Only at some compositions has ferromagnetic order been found but with T_C well below RT (nominal T_C ranging from 100 K[10] to 120 K[9] for $Fe_{90}Sc_{10}$ and a maximum of 220 K[9] for $Fe_{80}Sc_{20}$). As a consequence, it may be inferred that not even interfacial segregation and/or inhomogeneous elemental distributions could alone account for the ferromagnetism observed in the $Fe_{90}Sc_{10}$ nanoglass. Since the spectra of the ribbon and nanospheres are identical and show no magnetic order, only the formation of an interfacial region by joining the nanospheres leads to the observed order at RT. The size reduction alone (from (bulk) ribbon to nanospheres) does not give the same effect. In addition, the results of MS rule out bcc-Fe or Fe-oxides crystallites as an origin of the ferromagnetism.

Using molecular dynamics simulations, the general structural features of a model nanoglass can be identified. Şopu *et al.*,[5] have simulated the formation of a nanoglass by joining amorphous nanospheres (5 nm diameter) under high pressure and compared this to the structure of a melt-spun ribbon that was simulated by rapidly quenching from the melt. The atomic arrangements resulting from both simulations are displayed in Figs. 2(f) and 2(g). Even in the monoatomic case of Ge, the amorphous nanostructure is retained during the compaction process. Clearly, the simulations show two distinct regions: the "cores" of the consolidated nanoparticles and the regions of reduced density between them. Despite the differences in the interatomic potentials of Ge and the FeSc system, the structural features obtained from the simulation agree with the experimental results of STM in this study.

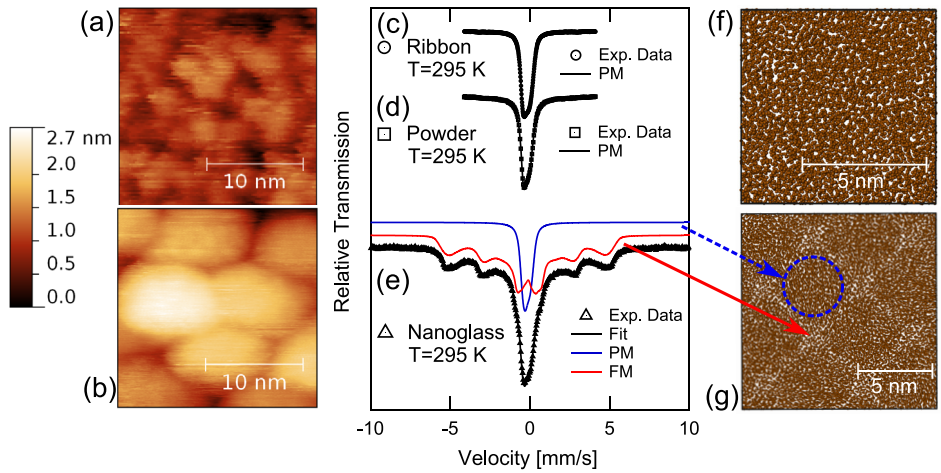

FIG. 2. Constant current STM image of the surface of (a) a polished melt-quenched ribbon and (b) a polished nanoglass sample, displaying a nano-granular structure. Mössbauer spectra at room temperature of (c) the melt-spun ribbon, (d) nanosphere powder prior to consolidation, and (e) the nanoglass. The melt-spun ribbon and the unconsolidated nanosphere powder exhibit the identical single line spectrum typical for paramagnetic materials. The nanoglass spectrum can be separated in a paramagnetic component (PM, dashed), with a spectral shape similar to the ribbon and the powder and a ferromagnetic (FM, continuous) component. This component consists of six lines that are a characteristic feature of ferromagnetic materials. (f) Molecular dynamics simulation of a melt-quenched Ge glass. (g) Molecular dynamics simulation of a Ge nanoglass, cf. Ref. 5. The arrows indicate the location of the two different components (FM and PM) of the Mössbauer spectrum in the nanoglass structure. The structure and density inside the region indicated by the circle corresponds to the paramagnetic component of the melt-spun ribbon shown in (c).

Moreover, Ghafari *et al.*, have shown by means of high energy X-ray diffraction that the number of Fe nearest neighbor atoms in the regions of reduced-density of the $Fe_{90}Sc_{10}$ nanoglasses is lowered by up to 15% as compared to that in melt-spun ribbons.[4] Fang *et al.*, have reported additional experimental evidence for the presence of regions of reduced density in $Fe_{25}Sc_{75}$ nanoglasses.[3] In this Sc rich nanoglass, an excess free volume in the interfaces between the glassy regions of at least 6% was revealed. In summary, all of the results reported so far seem to support the suggestion that a different amorphous structure is formed in glasses produced by consolidating nanometer-sized glassy spheres.

The fact that room temperature ferromagnetism is observed only if the $Fe_{90}Sc_{10}$ nanospheres are compacted (Fig. 2(e)) leads to the conclusion that the reduced-density regions create magnetic order, while the "dense" amorphous structure (as indicated by the arrows and the circle in Figs. 2(e) and 2(g)) remains partially paramagnetic. The difference between the magnetic properties of the two amorphous structures at RT, i.e., paramagnetic for the melt-spun glass and ferromagnetic for the nanoglass, is the most significant finding of our study: ferromagnetism is obtained by merely joining or compacting amorphous nanoparticles. However, note that the area of the sextet compared to the single line spectrum ($\sim$70%) is larger than what could reasonably be attributed to interface regions alone. Thus, the magnetic order in the interfaces extends inwards (into the primary nanoparticle) by exchange interactions and consequently results in a larger spectral fraction of the magnetically ordered component.

Low temperature measurements allow us to further investigate the magnetic ground state of the samples. As may be seen in Fig. 3, the M vs. H loops of the nanoglass and the melt-spun ribbon measured at 10 K show for both samples a typical hysteresis behavior and a small coercive field. At low temperature, the ribbon orders magnetically as well, with a magnetization of about 1.35(1) μ_B per Fe atom at an applied external field of 4.5 T, without achieving complete saturation at this field (note the strong slope of $M(H)$). In contrast, the nanoglass possesses a magnetization of about 1.74(2) μ_B per Fe atom at these fields, i.e., an increase of 29%. Such a magnetization value can only be achieved if a substantial fraction of the sample is ferromagnetic with less non-collinearity than it is the case for the ribbons. The magnetic state of both the ribbons and nanoglasses in field will be further discussed below.

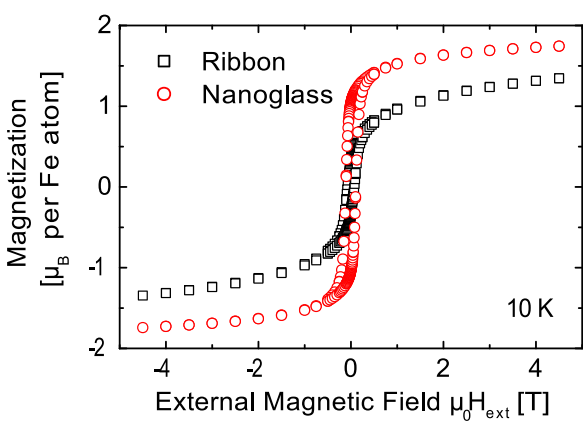

FIG. 3. Magnetization measurements at 10 K. The average magnetization increases in the nanoglass to 1.74(2) μ_B compared to 1.35(1) μ_B per Fe atom in the melt-spun ribbon. The error bars are smaller than the symbols.

The MS spectra of the ribbon at 4.5 K and the nanoglass measured at 10 K are given in Fig. 4. The spectrum for the ribbon is a simple magnetic hyperfine distribution[10] (not shown). For the nanoglass, there are two main components, one magnetic distribution similar in form to that of the melt-spun ribbon and a second distinct magnetic sextet, only present in the nanoglass. It exhibits a large magnetic hyperfine field B_{HF} of about 37.5 T with a spectral fraction of about 35%. By analogy to the room temperature results reported above, this spectral component is attributed to Fe-atoms located in the reduced-density regions (interface). (Furthermore, a fraction of bcc-Fe of less than 10% is also observed. This part must be superparamagnetic at RT as it is contained in the single line subspectrum rather than a distinct subspectrum with B_{HF} of about 33 T.)

Figure 5 shows the temperature dependence of the normalized average $B_{HF}(T)/B_{HF}(0)$ for core, interface, bcc-Fe and the ribbon sample on scale of $T^{3/2}$. The data are given over the temperature range where magnetic order is well defined. The data points are well described by a linear fit. Although the $T^{3/2}$ relation is only valid at low temperatures for crystalline materials, it has been used in amorphous materials to values up to 0.6 T_C.[15] The negative slopes of the linear fits decrease going from the melt-spun ribbon to the core to the interface subcomponent in the nanoglass. This is an indication of the strong exchange coupling in the interfaces, which also polarizes the core regions. The lowest slope

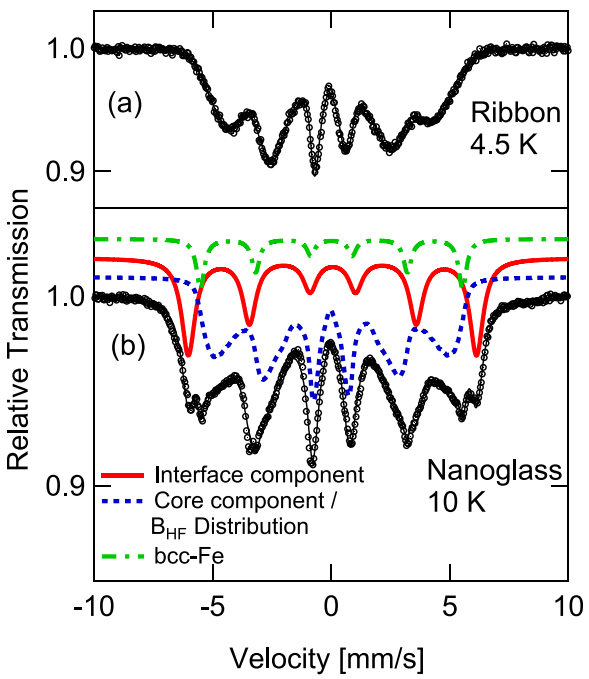

FIG. 4. Low temperature Mössbauer spectra of the (a) melt-spun ribbon and (b) nanoglass. The ribbon is fitted with a unimodal distribution of magnetic hyperfine fields B_{HF}. The nanoglass is fitted with one distribution of B_{HF} (dashed fitting curve), resembling the ribbon spectrum and two additional sextets. The continuous six line curve with a splitting of about 37.5 T represents the Fe atoms in the density reduced regions. Its spectral fraction reaches to about 35%. The dashed-dotted sextet is characteristic of bcc-Fe with a splitting of 34.3 T, with a spectral fraction of 9%.

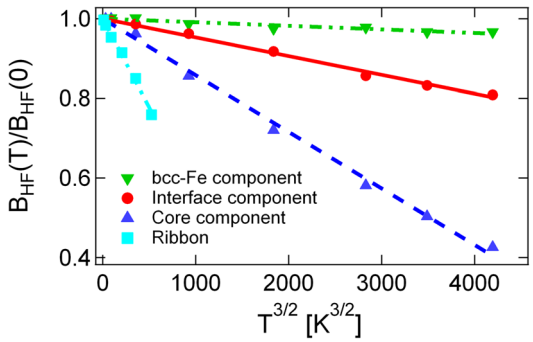

FIG. 5. Normalized hyperfine fields of the core distribution (average value), interface component, and bcc-Fe impurity (see Figs 2(e) and 4(b)). Results for the ribbon with similar composition are shown for comparison. $B_{HF}(0)$ is obtained by extrapolation.

is shown for the bcc Fe impurity (9%). Remarkable is that the core is magnetically ordered at temperatures (~200 K) well above the ordering temperature of the ribbon (100K), which is again proof for the strong interface/core exchange coupling. A similar effect was observed for fine iron precipitates in an amorphous FeZr matrix. The exchange-field of the iron crystallites penetrates into the residual amorphous matrix and increases the T_C of this phase.[16]

The in-field properties of the ribbons at low temperature have been investigated by Ghafari *et al.*,[17] and Ryan *et al.*,[18] While there are large differences in the approach in these studies (the first discussing a cluster glass state and the latter an asperomagnetic state), both agree that in the field range considered here, the Fe moments in the ribbons are non-collinear due to internal exchange interactions. Very high external magnetic fields (ca. 30 T) and an extrapolation $1/H \rightarrow 0$ are necessary to measure the spontaneous magnetization. Strong competing exchange interactions between moments prevent a full alignment in the direction of the external field. This non-collinearity is also seen by MS. A finite intensity of Mössbauer lines 2 and 5 remains in this range of external fields. This intensity depends on the angle Θ between the Mössbauer gamma ray and the hyperfine field as $4\sin^2\theta/(1+\cos^2\theta)$. This non-collinearity explains the slow approach to saturation of $M(H)$ for the ribbons.

The fact that the low temperature $M(H)$ of the nanoglass is much larger than that of the ribbons (in this range of external field) demonstrates that the ferromagnetism of the interfaces has strongly reduced the non-collinearity, even in the core regions. The slope of $M(H)$ for the nanoglass is also much smaller, consistent with a much faster approach to saturation and collinearity. In fact, the apparent saturation of $M(H)$ for the nanoglass is very similar to that for the ribbons at high external field.[18]

The magnetic state of 3d metallic systems is determined by the competition between exchange interactions, promoting electrons into parallel configurations, and the resulting increase in kinetic energy.[19] The study of ultrathin film structures has revealed especially for iron an extreme sensitivity to atomic volume (see Fig. 16 in Ref. 19 and Fig. 4 from Ref. 20). This sensitivity has been seen as well experimentally.[21] Generally, it is found that a decrease in atomic volume leads to a collapse of magnetic order in metals. Here we see this sensitivity to increased atomic volume in the strong ferromagnetism and increased T_C of the nanoglass interface layer, strong enough to affect the magnetic state of the enclosed amorphous core as well.

Moreover, Lorenz *et al.*,[22] have investigated the magnetic ground state of amorphous Fe as function of the atomic density by a tight-binding Hubbard Hamiltonian approach and observe a very sharp transition to collinear ferromagnetism as the density decreases. Compatible with this, we report heterogeneous collinear ferromagnetism in the nanoglass located in the low-density regions.

Many questions still need answering on this heterogeneous magnetic state, but it is clear that the ferromagnetism of the interface regions polarizes the core regions at low temperatures. The different hyperfine fields seen for the two regions indicate differences in electronic structure rather than in magnetic moment per iron atom. In addition to the remarkable enhanced magnetic properties reported in this paper, which are directly related to the modified amorphous structure, we anticipate that nanoglasses may possess other attractive properties. In fact, recently, some results indicate that nanoglasses exhibit altered mechanical,[3,23] biocompatible, and catalytic[11] properties.

This work was supported by the Deutsche Forschungsgemeinschaft (DFG) under contracts HA 1344/23-1 and HA 1344/28-1. The authors appreciate the support by A. Leon (KIT) and M. Stoica (IFW Dresden) for the preparation of the reference metallic glass sample. The authors are grateful to D. Şopu and K. Albe (TU Darmstadt) for providing the results of molecular dynamics simulations. They appreciate the helpful discussions with V. Provenzano (NIST Gaithersburg) and D. M. Eisele (MIT). One of the authors (H.H.) expresses his special thanks to the State of Hessen for an equipment grant at the TU Darmstadt. Support from the NES program at KIT (H.G.) and fellowships by the Alexander-von-Humboldt Foundation (T.F. and J.X.F.) are gratefully acknowledged.

[1]H. Gleiter, Prog. Mater. Sci. **33**, 223–315 (1989).
[2]J. Jing, A. Kramer, R. Birringer, H. Gleiter, and U. Gonser, J. Non-Cryst. Solids **113**, 167–170 (1989).
[3]J. X. Fang, U. Vainio, W. Puff, R. Würschum, X. L. Wang, D. Wang, M. Ghafari, F. Jiang, J. Sun, H. Hahn, and H. Gleiter, Nano Lett. **12**, 458–463 (2012).
[4]M. Ghafari, S. Kohara, H. Hahn, H. Gleiter, T. Feng, R. Witte, and S. Kamali, Appl. Phys. Lett. **100**, 133111 (2012).
[5]D. Sopu, K. Albe, Y. Ritter, and H. Gleiter, Appl. Phys. Lett. **94**, 191911 (2009).
[6]Y. Ritter, D. Sopu, H. Gleiter, and K. Albe, Acta Mater. **59**, 6588–6593 (2011).
[7]M. Ghafari, H. Hahn, H. Gleiter, Y. Sakurai, M. Itou, and S. Kamali, Appl. Phys. Lett. **101**, 243104 (2012).
[8]R. Birringer, H. Gleiter, H.-P. Klein, and P. Marquardt, Phys. Lett. A **102**, 365–369 (1984).
[9]M. Müller, M. Ghafari, S. H. Banihashemei, B. Stahl, and H. Hahn, Phys. Status Solidi A **189**, 1043–1049 (2002).
[10]R. Day, J. Dunlop, C. Foley, M. Ghafari, and H. Pask, Solid State Commun. **56**, 843–845 (1985).
[11]N. Chen, R. Frank, N. Asao, D. V. Louzguine-Luzgin, P. Sharma, J. Q. Wang, G. Q. Xie, Y. Ishikawa, N. Hatakeyama, Y. C. Lin, M. Esashi, Y. Yamamoto, and A. Inoue, Acta Mater. **59**, 6433 (2011).
[12]U. Geyer, U. von Hülsen, and P. Thiyagarajan, Appl. Phys. Lett. **70**, 1691 (1997).
[13]D. Wang, U. Geyer, and S. Schneider, J. Non-Cryst. Solids **221**, 222 (1997).

[14]A. I. Oreshkin, N. S. Maslova, V. N. Mantsevich, S. I. Oreshkin, S. V. Savinov, V. I. Panov, and D. V. Louzguine-Luzgin, JETP Lett. **94**, 58 (2011).
[15]C. L. Chien and R. Hasegawa, Phys. Rev. B **16**, 2115 (1977).
[16]K. Suzuki and J. M. Cadogan, J. Appl. Phys. **87**, 7097–7099 (2000).
[17]M. Ghafari, R. K. Day, J. B. Dunlop, and A. C. McGrath, J. Magn. Magn. Mater. **104**, 1668 (1992).
[18]D. H. Ryan, J. O. Ström-Olsen, and W. B. Muir, Phys. Rev. B **40**, 11208 (1989).
[19]C. A. F. Vaz, J. A. C. Bland, and G. Lauhoff, Rep. Prog. Phys. **71**, 056501 (2008).
[20]H. C. Herper, E. Hoffmann, and P. Entel, Phys. Rev. B **60**, 3839 (1999).
[21]W. Keune, A. Schatz, R. D. Ellerbrock, A. Fuest, K. Wilmers, and R. A. Brand, J. Appl. Phys. **79**, 4265 (1996).
[22]R. Lorenz and J. Hafner, J. Magn. Magn. Mater. **139**, 209 (1995).
[23]D. Şopu, Y. Ritter, H. Gleiter, and K. Albe, Phys. Rev. B **83**, 100202 (2011).